IAES International Journal of Artificial Intelligence (IJ-AI)
Vol. 15, No. 6, December 2026, pp. 5799~5809
ISSN: 2252-8938, DOI: 10.11591/ijai.v15.i6.pp5799-5809

A semantic segmentation-assisted deep ensemble framework for colon cancer classification

Euddla Narayanappa Srivani[1,2], Seshikala Gumastha[1]
[1]School of Electronics and Communication, REVA University, Bengaluru, India
[2]Department of Electronics and Communications, SJC Institute of Technology, Chickballapur, India

Article Info

Article history:

Received Jun 20, 2025
Revised Aug 19, 2026
Accepted Sep 19, 2026

Keywords:

Colon cancer detection
Criss-cross network
DenseNet121
Ensemble machine learning
Gray-level co-occurrence matrix
Hybrid deep ensemble
ResNet101

ABSTRACT

Accurate and automated diagnostic techniques are required to help clinical decision-making due to the increase in colorectal cancer cases worldwide. While current computer-aided diagnostic (CAD) approaches face challenges such as class imbalance, limited contextual comprehension, and convergence issues, manual diagnosis is often affected by human errors and inconsistencies. To address these challenges, this study proposes the criss-cross network (CCNet), a semantic segmentation-assisted deep spatio-textural feature ensemble learning framework for colon cancer detection and classification that is region of interest (ROI)-specific and aided by semantic segmentation. The proposed model uses fuzzy C-means (FCM) clustering based on the firefly algorithm to segment tissue sections using the lung and colon cancer histopathological image dataset (LC25000). Following the extraction of spatio-textural features using gray-level co-occurrence matrix (GLCM), residual network with 101 layers (ResNet101), and densely connected convolutional network with 121 layers (DenseNet121), feature fusion, principal component analysis (PCA) based selection, and Z-score normalization are performed. For final classification, a heterogeneous ensemble classifier with majority voting that combines support vector machine (SVM), decision tree (DT), naïve Bayes, random forest (RF), and extreme gradient boosting (XGBoost) is employed. With an accuracy of 99.37% in classifying colorectal images as benign or malignant, CCNet outperforms current techniques and demonstrates its efficacy and resilience for real-time colon cancer diagnosis.

This is an open access article under the CC BY-SA license.

Corresponding Author:

Euddla Narayanappa Srivani
School of Electronics and Communication, REVA University
Bangalore 560064, India
Email: vani.sri04@gmail.com

1. INTRODUCTION

The incidence of cancer has increased dramatically worldwide in recent years, and a notable increase in death rates has prompted the creation of more reliable and accurate computer-aided diagnostic (CAD) systems for early and efficient disease diagnosis. This increasing trend in cancer incidence has been caused by several causes, including dietary changes, urbanization, environmental pollution, and sedentary lifestyles. The unchecked proliferation of aberrant cells in particular body areas or throughout the body is what defines cancer [1]. To preserve tissue integrity and function, the human body, which is made up of trillions of cells, normally maintains a balanced cycle of cell creation and programmed death. On the other hand, if this equilibrium is upset, aberrant cells may develop and spread to neighboring tissues.

One characteristic of cancer cells is their capacity to spread and penetrate neighboring tissues, which increases the bulk of the afflicted areas [2]. Both benign and malignant tumors may form because of this invasive activity. In contrast to benign tumors, which often stay confined and do not metastasize, malignant tumors aggressively spread to nearby tissues and organs. Benign tumors are less dangerous, but when they grow in delicate areas like the brain, they can cause serious problems or even death [3].

The World Health Organization recently reported that over 20 million instances of cancer were reported worldwide in 2022, with an estimated 9.7 million deaths from the disease [4]. According to the survey, nearly 53.5 million people are anticipated to live for up to five years after receiving a diagnosis. It is estimated that one in five people will receive a cancer diagnosis at some time in their lives, which is concerning. With 2.5 million new instances of lung cancer in 2022—a 12.4% rise over prior years—lung and blood cancers have become the most common types. Similarly, colorectal cancer reached 1.9 million new cases, indicating a 9.6% annual increase, and breast cancer cases increased by 11.6% to 12.3 million [5].

The colorectum, or large intestine, is the last component of the human digestive system and is essential for the absorption of minerals and water from partially digested food, called chyme. Liquid chyme is transformed into solid feces during this process, which can take up to 16 hours [6]. It has a greater amount of goblet cells that secrete mucin, which helps with waste disposal, and it does not have villi as the small intestine does [7], [8]. The transverse colon, hepatic flexure, splenic flexure, descending colon (left colon), rectum, anal canal, sigmoid colon, and cecum (right colon or ascending colon) are the anatomical components that make up the large intestine. Polyps, which are abnormal growths that can eventually turn into cancer, are frequently the precursors of colorectal cancer, which develops when the cells lining the colon or rectum start to grow out of control. These polyps can reach the outer layers of the intestinal wall, but they usually start in the innermost layer.

Even though early detection is crucial, human error and complexity in traditional diagnostic techniques like tissue biopsy and manual assessment frequently result in worse than ideal outcomes. By automatically identifying and categorizing malignant tissues in histopathological and endoscopic pictures, computer vision and artificial intelligence (AI) technologies present viable alternatives in this regard. These image types have been used in several previous attempts to investigate machine learning models for colorectal cancer detection. However, the quality of the characteristics that are retrieved and the learning capabilities of the model have a major role in how well such systems function [5].

Conventional methods have used deep learning-based features [9] and handcrafted features including color, texture, shape, and structural patterns [10], including bag-of-features and local binary patterns. However, traditional deep learning models, such as long short-term memory (LSTM) [11] and convolutional neural network (CNN) [12], frequently concentrate on local features and find it difficult to capture contextual information. This leads to issues like gradient vanishing, exploding gradients, and insufficient handling of long-term dependencies. Model generalization is hampered by these issues, especially when working with intricate, non-linear datasets.

Due to manual histopathological evaluation limitations, misclassification, and delayed diagnosis, colorectal cancer continues to rank among the top causes of cancer-related death. Poor generalizability, class imbalance, insufficient feature representation, and inappropriate segmentation are common problems with current CAD systems. Furthermore, traditional deep learning models suffer from problems like gradient vanishing and overfitting and lack contextual awareness. These restrictions make it more difficult to identify cancerous tissues accurately and early. This study suggests a robust semantic segmentation-assisted, region of interest (ROI)-specific deep spatio-textural ensemble learning model for effective colon cancer detection and classification, driven by the requirement for a dependable, accurate, and automated diagnostic framework.

The key contributions of this paper are as follows:

i) Suggested a semantic segmentation based on firefly algorithm-based fuzzy c-means (FFCM) for accurate ROI extraction from colorectal histopathology images.
ii) Created a hybrid deep spatio-textural feature extraction system with the models of densely connected convolutional network with 121 layers (DenseNet121), residual network with 101 layers (ResNet101), and gray-level co-occurrence matrix (GLCM).
iii) Z-score normalization and principal component analysis (PCA) were used for feature reduction and the best possible model generalization.
iv) Developed a heterogeneous maximum voting model (MVM)-based ensemble classifier that outperformed existing state-of-the-art methods, achieving an accuracy of 99.27%.

The paper is further organized as section 2 gives insights into the literature survey. Section 3 elaborates the proposed methodology with related modules. Section 4 presents the experimental analysis and discussions and finally the paper is concluded in section 5.

2. RELATED WORKS

This section reviews recent state-of-the-art vision-based methods developed for colon cancer detection. Sena *et al.* [9] showed that segmentation-based preprocessing greatly increases the accuracy of colon cancer diagnosis, with improvements of about 15% observed. In addition to improving accuracy, this preprocessing phase lowers processing expenses and computational time, increasing the detection system's efficiency. The renowned visual geometry group (VGG) deep learning network was also used [13] to detect colon cancer. Their method produced favorable loss (0.44), sensitivity (95.10%), and specificity (92.76%) metrics in addition to a high accuracy of 93.48%. This enhancement demonstrates how deep convolutional networks outperform conventional CNNs in this field. A CNN framework based on transfer learning was proposed [14] to extract predictive characteristics from tissue slides of colorectal cancer. They achieved an outstanding 94% classification accuracy by training their algorithm using histopathology pictures to classify single-tissue areas. Iizuka *et al.* [15] created a hybrid method for classifying pictures of stomach and colon tissue that combines CNNs and recurrent neural networks (RNNs). Their model was able to classify pictures into adenocarcinoma, adenoma, or non-neoplastic categories. The usefulness of segmentation in conjunction with deep learning for colorectal cancer detection was further illustrated [16]. Their approach demonstrated the significance of region-specific segmentation by achieving an accuracy of 94.8% on histopathological cancer images and 99.9% on normal images.

Using a sizable dataset of 5,000 histopathological pictures, Hamida *et al.* [17] created a deep architecture that combines CNN and residual network (ResNet) components to identify and categorize colon cancer. The segmentation network (SegNet) architecture beat their ResNet-CNN model, which achieved 96.68% accuracy, with 98.66% accuracy. In a related method, Babu *et al.* [18] extracted characteristics from colon biopsy photos using transfer learning with pre-trained CNN models such as Inception-V3, VGG-16, and AlexNet. Bayesian-optimized support vector machines (SVMs) were used to classify these features, and Inception-V3 had the best accuracy of 96.5%. Tasnim *et al.* [19] used mobile network version 2 (MobileNetV2) in conjunction with CNNs enhanced with max-pooling and average-pooling layers to detect colon cancer. MobileNetV2 beat all of the CNN models with max-pooling and average pooling layers, with accuracies of 99.67% and 95.48%, respectively. In a similar vein, Sakr *et al.* [20] claimed that CNNs on histological pictures could diagnose colon cancer with an accuracy of 99.5%. CNNs were also utilized [21], who reported that their model achieved an even greater accuracy of 99.8% for the categorization of adenocarcinomas.

With a flawless accuracy of 100%, Talukder *et al.* [22] presented a hybrid ensemble feature model that merged machine learning classifiers with deep features taken from histopathology images for two-class categorization. To create predictive models, Bostanci *et al.* [11] investigated ribonucleic acid sequencing (RNA-seq) with contrasted deep learning models like 1D CNN, LSTM, and bidirectional long short-term memory (BiLSTM) with traditional machine learning algorithms like k-nearest neighbors (KNN), logistic model trees (LMT), random trees (RT), and random forest (RF). They found that CNN and BiLSTM models had somewhat higher accuracies of 97.67% and 98%, respectively, whereas classical machine learning models reached accuracies of up to 97.33%.

For detecting colon cancer using histopathological images, a variety of additional deep learning models have been put forth [23]. For example, Toğaçar [23] achieved a high accuracy of 99.69% by using DarkNet-19 as a feature extractor and then an SVM classifier. Handcrafted characteristics like color, texture, shape, and structural descriptors were retrieved [10] and then integrated with RF and DenseNet121 classifiers. For the classification of lung and colon cancer, this method produced an F1-score of 0.985 and accuracy, recall, and precision of 98.60%. A 45-layer deep CNN model was created [24], who reported a 99.75% accuracy rate. However, gradient vanishing issues could result from the deep architecture and heavy reliance on dropout layers, which could lower runtime accuracy.

The VGG-16 network was used [25] to identify colon cancer, with an accuracy of 88.03%. Multispectral colorectal tissue categorization based on active contour segmentation and CNNs was used [26], although their reliance on manual segmentation hampered their robustness and scalability. Using pre-processing techniques such as tissue composition extraction and image normalization, Kainz *et al.* [27] segmented and classified colon glands. They then used Object-Net and Separator-Net for gland segmentation and ROI-specific feature learning.

3. SYSTEM MODEL

The overall working of the proposed methodology is presented in Figure 1, that follows with detailed discussion of each module. The proposed framework presents a systematic approach for colon cancer classification using histopathological images from the LC25000 dataset. Initially, images undergo preprocessing, followed by FFCM-based segmentation to isolate relevant tissue regions. Features are extracted using GLCM, ResNet101, and DenseNet121 and integrated through feature fusion. PCA-based feature selection and normalization reduce redundancy and improve representation. Subsequently, SVM, RF, DT,

XGBoost, and extra trees (ET) classifiers are combined through an ensemble strategy to distinguish cancerous and normal tissues, followed by comprehensive performance evaluation.

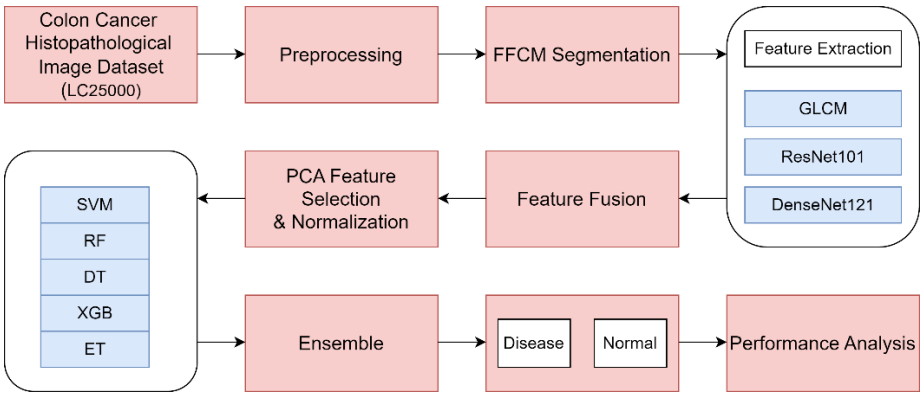

Figure 1. Proposed model for colon cancer detection

3.1. Data acquisition

In this work, colorectal histopathological images were taken into consideration. Specifically, the publicly available lung and colon cancer histopathological image dataset (LC25000) [28] was taken into consideration. The LC25000 dataset originally contains a total of 25,000 images. The original dataset represents a multi-class classification problem to classify input histopathological images as benign images or lung or colon cancer categories. However, since in this research the key focus is made on detecting colon cancer, the images represent colon adenocarcinoma and benign tissues. A total of 5,000 histopathological images were considered from each of these categories, and thus a whole sum of 10,000 images was considered for this research.

3.2. Data pre-processing

Standard pre-processing techniques, such as intensity and histogram equalization, and z-score normalization, were applied to histopathological pictures to address non-linear spatio-textural distributions. The criss-cross network (CCNet) used a 2D median filter for pixel normalization, contrast adaptive histogram equalization, and intensity equalization. The use of local contrast enhancement, as in (1).

$$p_n = \left(\frac{[u_w(p) - u_w(Min)]}{[u_w(Max) - u_w(Min)]}\right) \tag{1}$$

Where p is the pixel value, Min/Max are window intensities, and u_w is defined as in (2).

$$u_w = \left[1 + exp\left(\frac{f_w - p}{\sigma_w}\right)\right]^{-1} \tag{2}$$

With mean and standard deviation per window, as in (3) and (4).

$$f_w = \frac{1}{N^2}\sum_{(i,j)\in w(x,y)} p(i,j) \tag{3}$$

$$\sigma_w = \frac{1}{N^2}\sum_{(i,j)\in w(x,y)} (p(i,j) - f_w)^2 \tag{4}$$

Z-score normalization used image-wise mean (μ) and standard deviation (σ), as in (5).

$$x^i = \frac{(x - \mu)}{\sigma} \tag{5}$$

Images were resized to 320 × 320 and processed via FFCM for ROI-specific segmentation.

3.3. Firefly heuristic-based fuzzy C-means for cell segmentation

In this study, fuzzy membership functions are tuned using the Firefly algorithm to decrease inter-pixel distance in ROI segmentation. The system creates clusters according to light intensity, drawing inspiration from the firefly's adaptive movement and light-flashing behavior. It abides by three rules:

– Rule 1: regardless of gender, fireflies are drawn to one another by the intensity of the light.
– Rule 2: distance $I \propto \frac{1}{r^2}$, diminishes attraction, and a greater r^2 lowers the attraction coefficient β.
– Rule 3: the brightest firefly doesn't get attracted and moves at random.

The correlation between the cost-function and inter-pixel distance is used to find the centroid in N-dimensional space. Fireflies (pixels) are initially dispersed at random. Measurement of intensity disparity and pixel-by-pixel cluster formation are the next two processes. Pixel clusters with comparable intensity patterns are created when fireflies of different brightnesses attract one another. For firefly i, solution x_i and fitness $f(x_i)$ define intensity as (6).

$$I_i = f(x_i) 1 \leq i \leq n \tag{6}$$

Inter-firefly distance and attraction are as in (7) - (9).

$$r_{ij} = \|x_i - x_j\| \tag{7}$$

$$\beta(r) = \beta_0 exp^{\{-\gamma d(i,j)^2\}} \tag{8}$$

$$x_i(t+1) = x_i(x_j - x_i) + \alpha(rand - 0.5) \tag{9}$$

Cluster centroids are represented as in (10).

$$A = (s_1\{a_1 a_2, \ldots, a_d\}, s_2\{a_1 a_2, \ldots, a_d\}, s_3\{a_1 a_2, \ldots, a_d\}) \tag{10}$$

The Rosenbrock function is used as the objective function as in (11) and (12).

$$f(x,y) = (a-x)^2 + b(y-x)^2 \tag{11}$$

$$f(x) = \sum_{i=1}^{N-1} 100(x_{i+1} - x_i^2)^2 (1 - x_i)^2 \tag{12}$$

Segmentation output is red, green, and blue (RGB)-transformed for feature extraction and classification. An illustration of the segmentation output is given in Figure 2. Figure 2(a) shows the original colorectal histopathological images containing complex tissue structures and cellular variations. Figure 2(b) presents the corresponding FFCM-segmented outputs, where cell regions are clearly delineated and highlighted in RGB space, enabling precise ROI extraction and improved feature extraction for subsequent classification.

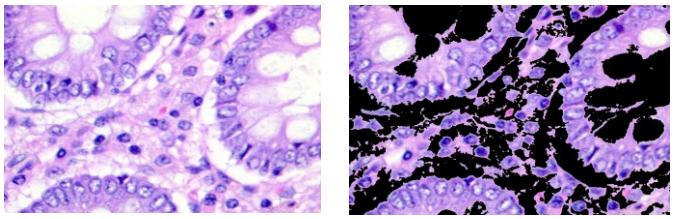

(a) (b)

Figure 2. FFCM segmentation output: (a) original histopathological images and (b) FFCM segmented cells from the input histopathological image

3.4. Region of interest specific deep spatio-textural ensemble feature extraction

The proposed method applies GLCM, ResNet101 and DenseNet121 deep models for feature extraction. This research hypothesizes that the amalgamation of the different feature sets, such as the spatio-textural features and high-dimensional, information rich deep features can yield superior learning accuracy and efficiency. More specifically, the proposed method applies the GLCM technique to extract the ROI-specific spatio-textural features, while ResNet101 and DenseNet121 are applied for learning and prediction.

3.4.1. Gray-level co-occurrence matrix feature

Learning resilience is improved by GLCM's varied orientational and spatio-textural properties, which set it apart from wavelet-based methods. RGB to grayscale (RGB2GRAY) is used to convert each ROI-specific image to grayscale. High-order statistical and textural properties are extracted using GLCM. To represent

spatial intensity differences, a probability matrix $P_{i,j}$ is generated using a pixel intensity matrix $I(x,y)$. As shown in (13), a symmetric matrix S is obtained and utilized to calculate P.

$$P_{i,j} = \frac{S_{i,j}}{\sum_{i,j=0}^{N-1} S_{i,j}} \tag{13}$$

From $P_{i,j}$, the following features are calculated, as in (14) to (25).

$$Homogeneity = \sum_{i,j=0}^{N-1} \frac{P_{i,j}}{1+(i-j)^2} \tag{14}$$

$$Contrast = \sum_{i,j=0}^{N-1} P_{i,j}\,(i-j)^2 \tag{15}$$

$$ASM = \sum_{i,j=0}^{N-1} {P_{i,j}}^2 \tag{16}$$

$$Energy = \sqrt{ASM_{i,j}} \tag{17}$$

$$Entropy = \sum_{i,j=0}^{N-1} P_{i,j}\left(-lnP_{i,j}\right) \tag{18}$$

$$\mu_i = \sum_{i,j}^{N-1} i\left(P_{i,j}\right) \tag{19}$$

$$\mu_j = \sum_{i,j}^{N-1} j\left(P_{i,j}\right) \tag{20}$$

$$\sigma_i^2 = \sum_{i,j}^{N-1} P_{i,j}(i-\mu_i)^2 \tag{21}$$

$$\sigma_j^2 = \sum_{i,j}^{N-1} P_{i,j}\left(j-\mu_j\right)^2 \tag{22}$$

$$\sigma_i = \sqrt{\sigma_i^2} \tag{23}$$

$$\sigma_j = \sqrt{\sigma_j^2} \tag{24}$$

$$Corelation = \sum_{i,j}^{N-1} P_{i,j}\left[\frac{(i-\mu_i)(j-\mu_j)}{\sqrt{\left(\sigma_i^2\right)\left(\sigma_j^2\right)}}\right] \tag{25}$$

Final GLCM feature vector as in (26).

$$Feat_{_\mathrm{GLCM}i} = \begin{bmatrix} ENE, ENT, CONT, Homogenity, CORR, \\ VAR, Mean, SD \end{bmatrix} \tag{26}$$

The extracted GLCM features ($Feat_{_\mathrm{GLCM}i}$) were later fused with the other feature models, including ResNet101 and DenseNet121. Details about these feature models are explained in the following subsection.

3.4.2. ResNet101 feature

The suggested model uses a hybrid residual ensemble structure for feature extraction utilizing ResNet101 and DenseNet121, in contrast to conventional CNNs. Input ROI-specific RGB histopathology pictures that have been scaled to 320 × 320 × 3 pixels are used by these deep networks to extract features. Batch normalization is applied to input images (27), where the pixel vector is indicated by $x(i,j)$.

$$\bar{x}(i,j) = \frac{x(i,j)}{127.5} - 1 \tag{27}$$

ResNet101 connects with residual blocks for fast convergence, governed by (28).

$$y = F(x,\{W_i\}) + x \tag{28}$$

In this case, $F(x,\{W_i\})$ is the residual mapping, while x and y are input/output feature vectors in 100 layers and 33 filters per layer. ResNet101 culminates in a dense layer that uses softmax and average pooling to produce fully connected features for learning and prediction.

3.4.3. DenseNet121 feature

To create a high-dimensional feature set, the suggested model uses a native CNN (ConvNet) architecture to extract hierarchical features utilizing several filters. DenseNet improves feature reuse and learning efficiency by allowing each layer to receive input from all layers that came before it. In particular, layer l receives the output of layer l - 1 as input, and layer l + 1 receives the output of layer l, according to the formula $X_1 = H_1(X_1 - 1)$, where H_1 is a composite function that includes batch normalization, rectified linear unit (ReLU), and pooling. To enable dense connectivity, DenseNet concatenates previous features $(X_0, X_1, \dots, X_{l-1})$ and uses them as input to layer l as in (29).

$$X_l = H_1([X_0, X_1, \dots, X_{l-1}]) \tag{29}$$

Here $(X_0, X_1, \dots, X_{l-1})$ represents the fused feature map. This dense connection design alleviates vanishing gradients, reduces computational cost, and improves feature informativeness. The model consists of four dense blocks connected by transition layers that include batch normalization, pooling, and clipped ReLU activation. Unlike standard ReLU, the clipped ReLU restricts activation values to a predefined ceiling, improving sensitivity to non-linear patterns. Finally, the extracted feature set $Feat_{DenseNet121}$ is passed through a global average pooling (GAP) layer and then flattened, yielding the final learnable feature vector for downstream tasks.

3.5. Deep spatio-textural feature fusion (ensemble)

Being a feature ensemble model, the GLCM feature $\left(Feat_{GLCM_i}\right)$, ResNet101 $\left(Feat_{_\text{ResNet101}}\right)$, and DenseNet121 feature $(Feat_{DenseNet121})$ were horizontally concatenated to generate an ensemble feature set. This process is depicted in (30) for further learning and classification.

$$Feat_{STDE} = [Feat_{GLCM_i};\ Feat_{_\text{ResNet101}};\ Feat_{DenseNet121}] \tag{30}$$

3.6. Principal component analysis feature selection and Z-score normalization

The suggested model uses CCNet over $Feat_{STDE}$ (30) to remove duplication while maintaining important information to solve the large dimensionality and computational expense that come from merging GLCM, ResNet101, and DenseNet121 features. Each feature set's principal components and eigenvalues are calculated using PCA. While some features are eliminated, those whose eigen distance is less than the mean principal component value (0.5) are kept. To reduce overfitting, the chosen features are subsequently normalized using z-score normalization. Each feature's μ and σ must be calculated, and the data must be transformed so that the standard deviation equals 1 and the mean becomes closer to zero using (31).

$$x^i = \frac{(x-\mu)}{\sigma} \tag{31}$$

The normalized characteristics are fed into a heterogeneous ensemble learning (HEL) framework, which performs consensus-based prediction and robust classification using the maximum voting ensemble (MVE) technique.

3.7. Heterogeneous ensemble learning-based classification

Individual machine learning classifiers frequently generate different results for the same input in classification tasks, indicating performance variability. The suggested model uses an ensemble learning strategy for two-class classification to overcome this. The suggested CCNet uses a HEL strategy by combining classifiers from various categories, including SVM for pattern mining, decision tree (DT) for rule-based logic, naïve Bayes for probabilistic modeling, and ensemble methods like RF and extreme gradient boosting (XGBoost), in contrast to traditional ensemble methods like RF, bagging, or boosting that mainly rely on DTs. The final prediction is decided by majority voting based on the highest-class score. These five classifiers work separately, assigning binary labels (1 for adenocarcinoma, 0 for benign).

4. EXPERIMENTAL RESULTS AND DISCUSSION

MATLAB 2022b was used to implement the CCNet model, which was then run on a system with an Intel i5 Processor operating at 3.2 GHz, 16 GB of RAM, and a standard central processing unit (CPU) environment. Key statistical parameters, such as accuracy, precision, recall, and F-measure, were used to assess the model's efficacy. Both intra-model and inter-model assessments were used to evaluate performance. To examine internal performance variances, different feature extraction methods and classifier combinations were explored in the intra-model evaluation. The suggested approach was compared to current colon cancer detection and classification techniques for inter-model evaluation to confirm its relative effectiveness.

4.1. Intra-model assessment

As previously said, this study sought to improve a number of elements, such as HEL-MVE-based classification, ROI segmentation, and ROI-focused deep spatio-textural ensemble feature extraction. Different feature extraction models, segmentation techniques, and classification algorithms were used in simulations to assess each component's efficacy. Finding out if the suggested segmentation method, feature extraction strategy, and classification technique work better in terms of accuracy and dependability than current state-of-the-art approaches was the main goal.

4.1.1. Segmentation characterization

The simulations were conducted under three different test conditions, first without segmentation, second with fuzzy C-means (FCM)-based segmentation, and third with the proposed FFCM-based segmentation. In the case of the simulation without segmentation, the original images were directly passed as input to the feature extraction. The other processes, such as PCA-based feature selection and z-score normalization, were applied in all test cases. The classification in all three simulation cases was done by using the HEL-MVE classifier. As depicted in Table 1, the colon cancer classification accuracy without any segmentation was measured as 94.17%, while precision, recall, and F-measure were obtained as 97.44%, 97.82%, and 0.97, respectively. Observing overall results, it can be inferred that the proposed FFCM model exhibits superior accuracy (99.37%) compared to the FCM segmentation-driven solution (96.22%). This result confirms the robustness of the proposed FFCM segmentation model to yield higher accuracy towards run-time significance.

Table 1. Segmentation assessment

Feature model	Accuracy (%)	Precision (%)	Recall (%)	F-measure
Without	94.17	97.44	97.82	0.97
FCM	96.22	97.42	98.12	0.97
FFCM	99.37	99.32	99.36	0.99

4.1.2. Feature assessment

Features from GLCM, ResNet101, and DenseNet121 were included in the classification trials in addition to the suggested deep spatio-textural ensemble features. The HEL-MVE ensemble classifier for binary classification was used to assess these. Energy, entropy, correlation, homogeneity, contrast, and other statistical and textural characteristics are captured by GLCM, which has 94.89% accuracy, 92% precision, 93.21% recall, and an F1-score of 0.92, as indicated in Table 2. The accuracy of HEL-MVE in conjunction with ResNet101 features was 96.38%. DenseNet121 produced an accuracy of 97.8%. Notably, with 99.37% accuracy and a 0.99 F1-score, the integrated feature set comprising GLCM, ResNet101, and DenseNet121 performed best, demonstrating the efficacy of the suggested model.

Table 2. Feature assessment

Feature model	Accuracy (%)	Precision (%)	Recall (%)	F-measure
GLCM	94.89	92.00	93.21	0.92
ResNet101	96.38	94.11	99.00	0.96
DenseNet121	97.79	99.19	95.82	0.98
Proposed	99.37	99.32	99.36	0.99

4.1.3. Classifier assessment

The simulation results obtained over the different (base) classifiers are shown in Table 3. As depicted in Table 3, the SVM base classifier shows an accuracy of 94.98%, precision 94.86%, recall 95.01%, and F-measure 0.94. The DT as base classifier yields the highest colon-cancer classification accuracy of 95.79%, precision 93.27%, recall 98.21%, and F-measure 0.95. The RF classifier, on the other hand, shows the colon cancer classification accuracy, precision, recall, and F-measure of 96.24%, 91.11%, 99.00%, and 0.96, respectively. The ET ensemble classifier depicts the colon cancer classification accuracy of 96.63%, precision 92.99%, recall 98.94%, and 0.99, respectively. The XGBoost classifier yielded the highest colon-cancer classification accuracy of 98.97%, precision 99.38%, recall 98.94%, and 0.99, respectively. The results show that the proposed HEL-MVE ensemble learning model exhibits colon-cancer classification accuracy of 99.27%, precision 99.32%, recall 99.36%, and an F-measure of 0.99. The overall results show and confirm that the proposed HEL-MVE ensemble learning model performs superior to the other machine learning classifiers.

Table 3. Classification assessment

Classifier	Accuracy (%)	Precision (%)	Recall (%)	F-measure
SVM	94.98	94.86	95.01	0.94
DT	95.79	93.27	98.21	0.95
RF	96.24	91.11	99.00	0.96
ET	96.63	92.99	98.71	0.96
XGBoost	98.97	99.38	98.94	0.99
HEL-MVE	99.27	99.32	99.36	0.99

4.2. Inter-model assessment

To assess the relative efficiency of the proposed CCNet model towards colon cancer detection and classification, the performance is compared with the other existing methods as well. A snippet of the relative performance by the other colon cancer detection methods and the proposed CCNet model is given in Table 4. Observing the results, it can easily be visualized that the proposed CCNet model exhibits superior than the majority of the state-of-arts. To be noted, despite the fact that the DNN model with RF ensemble learning model exhibited an accuracy of 100%; however, it lacks generalizability. The hybrid features encompassing the CNN and MobileNetV2 [19] exhibited the highest accuracy of 97.49%; yet, it falls below the proposed CCNet model, which shows the average accuracy of 99.27%. On the other hand, the active contour segmentation assisted CNN feature learning method yielded an accuracy of 90%. On the contrary, the proposed CCNet model that embodied FFCM segmentation followed by the hybrid deep feature (GLCM + ResNet101 and DenseNet121) and HEL-MVE ensemble classification yielded superior accuracy and reliability towards scalable colon-cancer detection and classification. In comparison to other deep models like CNN [14], [19]–[21], [24], the proposed CCNet model performs superior (99.27%). It confirms the superiority and robustness of the proposed model towards run-time scalable colon cancer detection and classification.

Table 4. Performance comparison of the proposed CCNet and existing approaches

Methods	Accuracy (%)
VGGNet [13]	93.48
CNN [14]	94.00
RNNs [15]	93.50
DNN with segmentation [16]	94.90
ResNet and CNN [17]	98.66
Inception-V3, VGG-16, and AlexNet + Bayesian SVM [18]	96.50
CNN and MobileNetV2 [19]	97.49
CNN [20]	99.50
CNN [21]	99.80
DNN + RF [22]	100.00
BiLSTM [11]	98.00
DarkNet-19 + SVM [23]	99.69
DenseNet-121 and RF [10]	98.60
CNN [24]	99.75
VGG-16 [25]	88.03
CNN + active contour segmentation [26]	90.00
Proposed CCNet	99.27

5. CONCLUSION

A segmentation-assisted ROI-specific deep ensemble learning system for colon cancer detection was introduced in this paper. FFCM was used to segment pre-processed histopathology pictures without the need for human interaction. After mapping the segmented areas to RGB, GLCM, ResNet101, and DenseNet121 were used to extract features. A HEL model that combined SVM, DT, RF, ET, and XGBoost was used to concatenate, normalize, and classify these features. Binary classification was determined by majority voting. CCNet outperformed current techniques with an accuracy of 99.27% and over 99% in precision, recall, and F1-score. The development of lightweight segmentation and feature extraction modules appropriate for real-time applications will be the main goal of future attempts to increase computing efficiency.

ACKNOWLEDGMENTS

The authors warmly acknowledge the Vision Group on Science and Technology, Govt. of Karnataka, and REVA University, Bengaluru, Karnataka, for providing the facilities required to carry out the research. The School of Electronics and Communication Engineering, REVA University, is also acknowledged for supporting this work.

FUNDING INFORMATION

The support extended by VGST, Govt. of Karnataka, in sponsoring this research with software tools under project no. KSTePS/VGST/GRD-684/KFIST(LI)/2018 is also gratefully acknowledged.

AUTHOR CONTRIBUTIONS STATEMENT

This journal uses the Contributor Roles Taxonomy (CRediT) to recognize individual author contributions, reduce authorship disputes, and facilitate collaboration.

Name of Author	C	M	So	Va	Fo	I	R	D	O	E	Vi	Su	P	Fu
Euddla Narayanappa Srivani	✓	✓	✓	✓	✓	✓		✓	✓	✓	✓			
Seshikala Gumastha	✓	✓		✓			✓			✓	✓	✓	✓	✓

C : **C**onceptualization
M : **M**ethodology
So : **So**ftware
Va : **Va**lidation
Fo : **Fo**rmal analysis
I : **I**nvestigation
R : **R**esources
D : **D**ata Curation
O : Writing - **O**riginal Draft
E : Writing - Review & **E**diting
Vi : **Vi**sualization
Su : **Su**pervision
P : **P**roject administration
Fu : **Fu**nding acquisition

CONFLICT OF INTEREST STATEMENT

The authors declare that they have no known financial, personal, professional, or other competing interests that could have influenced the research reported in this paper.

DATA AVAILABILITY

The data supporting this study are based on the publicly available research, reference [28].

REFERENCES

[1] F. Bray *et al.*, "Global cancer statistics 2022: GLOBOCAN estimates of incidence and mortality worldwide for 36 cancers in 185 countries," *CA: A Cancer Journal for Clinicians*, vol. 74, no. 3, pp. 229–263, May 2024, doi: 10.3322/caac.21834.
[2] R. A. Weinberg, "How cancer arises," *Scientific American*, vol. 275, no. 3, pp. 62–70, Sep. 1996, doi: 10.1038/scientificamerican0996-62.
[3] National Cancer Institute, "What is cancer?," *cancer.gov*, 2024. Accessed: Jun. 10, 2024. [Online]. Available: https://www.cancer.gov/about-cancer/understanding/what-is-cancer
[4] World Health Organization, "Global cancer burden growing, amidst mounting need for services," *WHO.int*, 2024. Accessed: Jun. 10, 2024. [Online]. Available: https://www.who.int/news/item/01-02-2024-global-cancer-burden-growing--amidst-mounting-need-for-services
[5] N. Shahadat, R. Lama, and A. Nguyen, "Lung and colon cancer detection using a deep AI model," *Cancers*, vol. 16, no. 22, Nov. 2024, doi: 10.3390/cancers16223879.
[6] A. Karthikeyan, S. Jothilakshmi, and S. Suthir, "Colorectal cancer detection based on convolutional neural networks (CNN) and ranking algorithm," *Measurement: Sensors*, vol. 31, Feb. 2024, doi: 10.1016/j.measen.2023.100976.
[7] M. M. Isfahani *et al.*, "Population attributable fraction of dietary risk factors for cancer mortality with a focus on gastrointestinal cancers in a population based cohort study," *Scientific Reports*, vol. 15, no. 1, Feb. 2025, doi: 10.1038/s41598-025-89183-x.
[8] T. K. Noah, B. Donahue, and N. F. Shroyer, "Intestinal development and differentiation," *Experimental Cell Research*, vol. 317, no. 19, pp. 2702–2710, Nov. 2011, doi: 10.1016/j.yexcr.2011.09.006.
[9] P. Sena, R. Fioresi, F. Faglioni, L. Losi, G. Faglioni, and L. Roncucci, "Deep learning techniques for detecting preneoplastic and neoplastic lesions in human colorectal histological images," *Oncology Letters*, vol. 18, no. 6, pp. 6101–6107, Sep. 2019, doi: 10.3892/ol.2019.10928.
[10] N. Kumar, M. Sharma, V. P. Singh, C. Madan, and S. Mehandia, "An empirical study of handcrafted and dense feature extraction techniques for lung and colon cancer classification from histopathological images," *Biomedical Signal Processing and Control*, vol. 75, May 2022, doi: 10.1016/j.bspc.2022.103596.
[11] E. Bostanci, E. Kocak, M. Unal, M. S. Guzel, K. Acici, and T. Asuroglu, "Machine learning analysis of RNA-seq data for diagnostic and prognostic prediction of colon cancer," *Sensors*, vol. 23, no. 6, Mar. 2023, doi: 10.3390/s23063080.
[12] H. Alqahtani, E. Alabdulkreem, F. A. Alotaibi, M. M. Alnfiai, C. Singla, and A. S. Salama, "Improved water strider algorithm with convolutional autoencoder for lung and colon cancer detection on histopathological images," *IEEE Access*, vol. 12, pp. 949–956, 2024, doi: 10.1109/ACCESS.2023.3346894.
[13] H. Yoon *et al.*, "Tumor identification in colorectal histology images using a convolutional neural network," *Journal of Digital Imaging*, vol. 32, no. 1, pp. 131–140, Feb. 2019, doi: 10.1007/s10278-018-0112-9.
[14] J. N. Kather *et al.*, "Predicting survival from colorectal cancer histology slides using deep learning: a retrospective multicenter study," *PLOS Medicine*, vol. 16, no. 1, Jan. 2019, doi: 10.1371/journal.pmed.1002730.
[15] O. Iizuka, F. Kanavati, K. Kato, M. Rambeau, K. Arihiro, and M. Tsuneki, "Deep learning models for histopathological classification of gastric and colonic epithelial tumours," *Scientific Reports*, vol. 10, no. 1, Jan. 2020, doi: 10.1038/s41598-020-58467-9.

[16] L. Xu *et al.*, "Colorectal cancer detection based on deep learning," *Journal of Pathology Informatics*, vol. 11, no. 1, Jan. 2020, doi: 10.4103/jpi.jpi_68_19.
[17] A. B. Hamida *et al.*, "Deep learning for colon cancer histopathological images analysis," *Computers in Biology and Medicine*, vol. 136, Sep. 2021, doi: 10.1016/j.compbiomed.2021.104730.
[18] T. Babu, T. Singh, D. Gupta, and S. Hameed, "Colon cancer prediction on histological images using deep learning features and Bayesian optimized SVM," *Journal of Intelligent & Fuzzy Systems*, vol. 41, no. 5, pp. 5275–5286, Nov. 2021, doi: 10.3233/JIFS-189850.
[19] Z. Tasnim *et al.*, "Deep learning predictive model for colon cancer patient using CNN-based classification," *International Journal of Advanced Computer Science and Applications*, vol. 12, no. 8, 2021, doi: 10.14569/IJACSA.2021.0120880.
[20] A. S. Sakr, N. F. Soliman, M. S. Al-Gaashani, P. Pławiak, A. A. Ateya, and M. Hammad, "An efficient deep learning approach for colon cancer detection," *Applied Sciences*, vol. 12, no. 17, Aug. 2022, doi: 10.3390/app12178450.
[21] M. I. Hasan, M. S. Ali, M. H. Rahman, and M. K. Islam, "Automated detection and characterization of colon cancer with deep convolutional neural networks," *Journal of Healthcare Engineering*, vol. 2022, pp. 1–12, Aug. 2022, doi: 10.1155/2022/5269913.
[22] M. A. Talukder, M. M. Islam, M. A. Uddin, A. Akhter, K. F. Hasan, and M. A. Moni, "Machine learning-based lung and colon cancer detection using deep feature extraction and ensemble learning," *Expert Systems with Applications*, vol. 205, Nov. 2022, doi: 10.1016/j.eswa.2022.117695.
[23] M. Toğaçar, "Disease type detection in lung and colon cancer images using the complement approach of inefficient sets," *Computers in Biology and Medicine*, vol. 137, Oct. 2021, doi: 10.1016/j.compbiomed.2021.104827.
[24] M. Yildirim and A. Cinar, "Classification with respect to colon adenocarcinoma and colon benign tissue of colon histopathological images with a new CNN model: MA_ColonNET," *International Journal of Imaging Systems and Technology*, vol. 32, no. 1, pp. 155–162, Jan. 2022, doi: 10.1002/ima.22623.
[25] N. Bayramoglu and J. Heikkilä, "Transfer learning for cell nuclei classification in histopathology images," in *Computer Vision – ECCV 2016 Workshops*, Cham: Springer, 2016, pp. 532–539, doi: 10.1007/978-3-319-49409-8_46.
[26] H. H.-Hassan, A. Chaddad, Y. Harkouss, C. Desrosiers, M. Toews, and C. Tanougast, "Classifications of multispectral colorectal cancer tissues using convolution neural network," *Journal of Pathology Informatics*, vol. 8, no. 1, Jan. 2017, doi: 10.4103/jpi.jpi_47_16.
[27] P. Kainz, M. Pfeiffer, and M. Urschler, "Segmentation and classification of colon glands with deep convolutional neural networks and total variation regularization," *PeerJ*, vol. 5, Oct. 2017, doi: 10.7717/peerj.3874.
[28] M. Al-Jabbar, M. Alshahrani, E. M. Senan, and I. A. Ahmed, "Histopathological analysis for detecting lung and colon cancer malignancies using hybrid systems with fused features," *Bioengineering*, vol. 10, no. 3, Mar. 2023, doi: 10.3390/bioengineering10030383.

BIOGRAPHIES OF AUTHORS



Euddla Narayanappa Srivani is working as an assistant professor in the Department of Electronics and Communication Engineering at SJC Institute of Technology and has 13 years of teaching experience. She received her B.Tech. degree in Electronics and Communication Engineering from BIT Institute of Technology, Jawaharlal Nehru Technological University Hyderabad, Hindupur. She completed her M.Tech. degree in Embedded Systems from St. Mary's College of Engineering, Jawaharlal Nehru Technological University Hyderabad. She is currently pursuing her Ph.D. in Electronics and Communication Engineering at REVA University, Bengaluru. She has published papers in referred international journals and has been granted two patents. She has received several best paper awards at various international conferences. Six Karnataka State Council for Science and Technology funded projects have been sanctioned to her. Her areas of research include image processing and embedded systems. She is an active member of IETE, IEI, and ISTE. She can be contacted at email: vani.sri04@gmail.com.



Seshikala Gumastha is a professor in the School of Electronics and Communication Engineering at REVA University, Bengaluru, India, with 29 years of teaching and research experience. She holds a Ph.D. and specializes in biomedical signal processing with interests in image processing and signal processing. She has organized FDPs, workshops, conferences, and seminars. She has authored 15 refereed journal publications and 25 conference papers, contributed 3 book chapters, and held 4 patents published. She has supervised 40+ UG/PG projects, guided 5 Ph.D. scholars, and is currently guiding 6 Ph.D. candidates. She has also secured one funded research project under Vision Group on Science and Technology of 20L and received the best researcher award in 2018 and 2021. She can be contacted at email: seshikala.g@reva.edu.in.